Magnetic Resonance in Medicine 45:376–382 (2001)

High-Temperature Superconducting Surface Coil for In Vivo Microimaging of the Human Skin

Jean-Christophe Ginefri,[1*] Luc Darrasse,[1] and Paul Crozat[2]

A small, high-temperature superconducting (HTS) surface coil was used to improve the signal-to-noise ratio (SNR) for in vivo human skin microscopy at 1.5 T. The internal noise of the conventional copper coil limits the SNR for this application. Inductive measurements of the HTS coil parameters indicated that at 77 K its internal noise contributed about 4% of the total noise, and the predicted SNR gain was about 3.2-fold over that of a room-temperature copper coil. In vivo images of the human skin produced with the HTS coil showed highly resolved details and a 3.7-fold improvement in SNR over that obtained with the room-temperature copper coil. Magn Reson Med 45:376–382, 2001. © 2001 Wiley-Liss, Inc.

Key words: superconducting; RF resonator; MR microimaging; skin; in vivo

The signal-to-noise ratio (SNR) is most important in biomedical NMR applications, and it must be maximized to obtain high spatial resolution with a conveniently short acquisition time. The main sources of noise in a carefully designed NMR coil are the internal noise of the coil itself and the noise inductively coupled to the coil by the sample (1). The induced noise is the dominant one in routine MRI applications, using large copper coils at room temperature. However, this decreases more rapidly than the internal noise when the coil size and the NMR frequency are reduced. Thus, the internal noise of the room-temperature coil may be considerably greater than the sample-induced noise in some specific MRI applications. This is the case for low-field MRI (2–4), high-field microscopy with small and nonconducting samples (5–9), and clinical imaging at intermediate field strengths (0.5–1.5 T) with small coils (10,11). This study concerns in vivo microimaging of the human skin in a whole-body MRI system at 1.5 T.

The SNR can be improved by reducing the thermal noise of the coil by using a high-temperature superconducting (HTS) coil, which may have a quality factor (Q) at liquid nitrogen temperature (77 K) about 3 orders of magnitude better than the Q of an equivalent copper coil at room temperature. The use of HTS coils in MRI has already improved the SNR for in vivo imaging at low-field strengths (3,4) and for in vitro microscopy at high-field strengths (5,7). Recent in vivo studies on animals using superconducting coils in NMR microscopes at 2 T (8) and 9.4 T (9) have also shown substantially better SNR than copper coils at room temperature. However, no significant improvements using HTS coils have been reported so far in MR applications on humans using the most current clinical system in the intermediate field range. The only report of an improved SNR by cryogenic means in this range was obtained by Wright et al. (10) using a small copper coil. They used a surface copper coil with a 10-mm radius cooled to 77 K to obtain in vivo images of the human finger at 1.5 T. We have employed an HTS surface coil with a mean radius of 6 mm that was recently designed in our laboratory (12).

THEORY

The actual contribution of the coil to the SNR at a given field strength is expressed by (1):

$$\mathrm{SNR} \propto \frac{b_1}{\sqrt{R_c T_c + R_s T_s}} \qquad [1]$$

where b_1 is the induction coefficient that represents the magnetic field produced by the coil per supplied unit current when used as an emission coil. R_c and T_c are the internal resistance and the temperature of the coil, respectively; T_s is the sample temperature; and R_s is the equivalent sample resistance inductively coupled in the coil.

The contributions of the noise sources can be compared by evaluating R_c (1) and R_s (13) in the case of a single-turn circular coil applied at the surface of a semi-infinite sample with a homogenous conductivity σ using the expressions:

$$R_c = \sqrt{\frac{\rho_c(T_c)\mu_0\,\omega_0}{2}}\,\frac{\xi a}{r}, \qquad [2]$$

$$R_s \approx \frac{1}{3}\,\sigma\mu_0^2\,\omega_0^2 a^3, \qquad [3]$$

where a is the radius of the RF coil, r is the radius of the coil conductor, μ_0 is the permeability of the free space, ρ_c is the conductor resistivity, and ω_0 is the Larmor angular frequency. ξ is the proximity effect factor; for a carefully designed RF coil, the ratio $\xi a/r$ is on the order of 40 (14). For the numerical calculation, we considered the resistivity of standard copper given as a function of T_c at a residual resistivity ratio (RRR) of 20 (15), and the average conductivity of the skin was set at 0.5 $S.m^{-1}$ (16). The limit at which the sample-induced noise R_sT_s becomes equal to the internal noise of the coil R_cT_c (4,17) is shown in Fig. 1. The figure also shows the theoretical limit where R_sT_s is equal to R_cT_c, in the case of a single-turn HTS coil made of YBaCuO. This curve was obtained using the surface resistance value of YBaCuO at 52 MHz (12) and assuming a ω^2

[1]Unité de Recherche en Résonance Magnétique Médicale, Université Paris-Sud, Orsay, France.

[2]Institut d'Électronique Fondamentale, Université Paris-Sud, Orsay, France.

Grant sponsor: French Ministry of Research.

*Correspondence to: Jean-Christophe Ginefri, U2R2M (CNRS ESA 8081), Bâtiment 220, Université Paris-Sud, F91405 Orsay, France.
E-mail: ginefri@u2r2m.u-psud.fr

Received 21 August 2000; revised 8 November 2000; accepted 20 November 2000.

© 2001 Wiley-Liss, Inc.

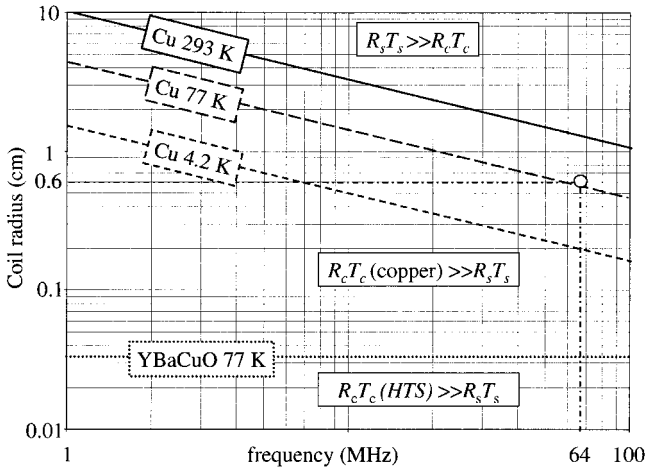

FIG. 1. Equality of the induced noise RsTs and the internal noise RcTc as a function of the coil radius and the ^{1}H Larmor frequency, for a copper coil at different temperatures (293 K, 77 K, and 4.2 K) and for a YBaCuO surface coil at 77 K. Computation was done using $\xi a/r = 44.5$, $\sigma = 0.5$ S.m^{-1}.

dependence of the superconducting losses. The influence of the magnetic field on the HTS properties was not taken into account for the calculation.

The internal losses of a conventional copper coil of 6-mm radius at 64 MHz at room temperature far exceed the induced losses (Fig. 1). Cooling such a copper coil down to 77 K results in the induced losses becoming dominant. However, the internal noise still contributes over half the SNR limitation. While cooling the copper coil to a very low temperature is required to make the internal losses negligible, the SNR with an HTS coil cooled to 77 K is not limited by internal losses. Consequently, an HTS coil should provide a significant SNR gain in our application.

MATERIALS AND METHODS

Coils

The HTS surface coil is based on a multiturn transmission line resonator design (12,18) with inner and outer radii of 4.5 and 7.3 mm, respectively. The resonator is made of two YBaCuO spirals (five circular loops) deposited on both surfaces of a lanthanum aluminate substrate (Fig. 2). It was made by Thomson-L.C.R. (Corbeville, France) (19), including the YBaCuO film deposition and etching. It was cooled to the temperature of liquid nitrogen using an NMR-dedicated cryostat (Desert Cryogenics, LLC, Tucson, AZ). The resonator was mounted on a sapphire plate (500 μm thick) in the secondary vacuum chamber of the cryostat, and the sapphire plate was connected to a sapphire rod immersed in a liquid nitrogen reservoir. The minimum distance allowed by the cryogenic insulation between the body surface and the resonator was 1 mm. In practice we used a spacing of 2 mm. Temperatures above and below 77 K were obtained by pressurizing and depressurizing the nitrogen reservoir.

The HTS resonator, at 77 K and at the magnitude of the earth's magnetic field, had an unloaded Q over 30000 and a resonance frequency of 63.985 MHz. It was accurately retuned to the frequency of the MRI system (63.835 MHz). The thermal dependence of the resonance frequency was derived from previous measurements (12) (Fig. 3). A shift of 0.1 K causes a frequency shift of about 500 Hz at around 77 K. A resonance frequency drift of less than 2 KHz can be maintained for approximately 1 hr, depending on the thermal stability of the cryostat. The HTS coil losses also depend on the temperature. However, a temperature shift of 1 K decreased the unloaded Q by less than 0.1% when the HTS coil was cooled to below 85 K. Therefore, the HTS coil could be operated at around 77 K without the need for a temperature-stabilization loop.

Coarse tuning was done by placing a thin dielectric sheet (PTFE, 123 μm thick) to partially overlap the YBaCuO strips on one side of the resonator. The dielectric sheet decreases the characteristic impedance of the resonator and lowers the resonance frequency. This does not significantly decrease the Q and is particularly suitable for HTS coils. We obtained frequency shifts of several MHz with sapphire, i.e., with a dielectric material of high permitivity and low loss tangent. The coil was finely tuned without opening the cryostat by placing a short-circuited copper loop (of the same mean radius as the HTS coil) on the outside of the cryostat window (Fig. 4). The copper loop decreases the equivalent inductance of the HTS coil, and therefore increases the resonance frequency. The tuning range with no significant degradation of the Q was limited to 150 KHz.

The HTS coil was matched to the standard preamplifier of the MRI unit via a parallel-resonant copper loop tuned at 63.9 MHz and inductively coupled to the HTS resonator (Fig. 4). The distance from the matching loop to the resonator was adjusted to reach the standard 50 Ω impedance.

We evaluated the improvement in SNR due to the HTS coil using a single-turn circular copper coil built with the same mean radius (0.6 mm) as the HTS coil. The coil is made of a strip of copper (2 mm wide) deposited on a 0.5-mm-thick PTFE substrate. The coil was tuned using two chip capacitors (ATC 100B, American Technical Ceramics, NY) connected in parallel to the copper loop, and it was matched to the preamplifier using a standard series-capacitance scheme. The unloaded Q was 101 at 63.840 MHz.

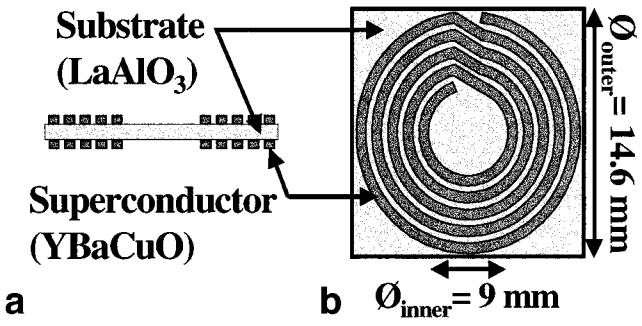

FIG. 2. Geometry of the HTS resonator. As shown in the cross section (**a**), the coil consists of two YBaCuO transmission lines separated by a dielectric sheet (lanthanum aluminate, 500 μm thick). The top view (**b**) shows the transmission lines geometry, made of five-turn circular loops with inner and outer radii of 4.5 and 7.3 mm, respectively.

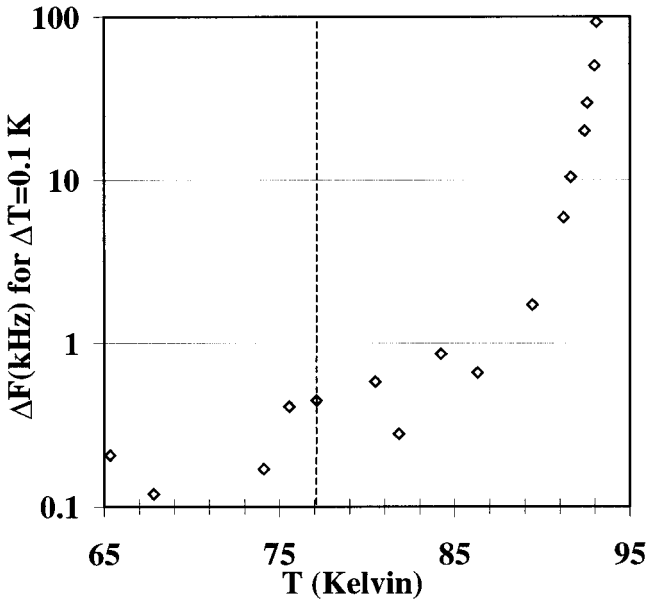

FIG. 3. Drift of the resonance frequency induced by a 0.1 K temperature shift as a function of the operating temperature.

Evaluation of Coil Efficiency With Inductive Measurements

We measured the resonance frequency and the Q factor of the HTS coil at static magnetic field strengths of from the earth field amplitude to 1.5 T. The applied magnetic field increases the losses within the HTS material (20) and shifts down the resonance frequency of the resonator, since the London penetration depth is increased (21). Measurements were made using the fringing field along the longitudinal axis of the MRI magnet. As HTS materials are strongly anisotropic (22), measurements were done for three orientations of the CuO layers in the static magnetic field. The CuO layers were parallel to the resonator plane in our system.

We predicted the HTS coil performance under imaging conditions by computing the SNR defined by Eq. [1] with measured values of the induction coefficient b_1, of the internal resistance R_c and of the inductively coupled resistance R_s.

R_c was extracted from the measurement of the unloaded quality factor (Q_{unloaded}) using the expression:

$$R_c = \frac{L\omega_0}{Q_{\text{unloaded}}}, \qquad [4]$$

where L is the equivalent inductance of the coil and ω_0 its angular resonance frequency.

R_s was obtained from the measured loaded and unloaded Q factors using the following formula (23):

$$R_s = \frac{L\omega_0(Q_{\text{unloaded}} - Q_{\text{loaded}})}{Q_{\text{unloaded}}Q_{\text{loaded}}}. \qquad [5]$$

The induction coefficient b_1 was measured on the coil axis using the inductive probe method (24). The Q factors were measured using a dual coupling technique (25) and an HP4195 network analyzer.

Imaging Experiments

Imaging was performed on a 1.5 T whole-body NMR scanner (Signa system, GE). The standard gradients of the whole-body scanner delivered a maximum gradient of 22 mT/m with a rise time of 288 μs. Skin microscopy requires an enhanced spatial resolution mainly perpendicular to the skin surface, since the skin consists of layered structures (11,26). We used an anisotropic 2D spin-echo sequence with a slice thickness of 900 μm; a pixel size of 40 μm in the read direction, perpendicular to the skin surface; and a pixel size of 80 μm in the phase-encoding direction. Both the HTS and the copper coil were used in transmit-receive mode. The latter mode was the only practicable one with the HTS coil due to the nonlinear behavior at current transmitted-power levels (8). The optimum transmitted power was set with either coil in order to maximize the signal amplitude from the epidermis using prescan profiles. The optimum level was typically 10 dB lower with the HTS coil than with the copper coil.

RESULTS

Resonance Frequency and the Q Factor

The influence of the magnetic field on the unloaded Q of the HTS coil for the three orientations of the CuO layers is shown in Fig. 5. The unloaded Q of the HTS coil decreased to 11000 at the center of the 1.5 T magnet when the CuO layers were parallel to the magnetic field, i.e., in the normal coil orientation when imaging. The resonance frequency was about 30 KHz lower than the resonance frequency at zero field. The Q value was about 1100 and the frequency shift was about 140 KHz with a perpendicular orientation. An uncorrect alignment of the coil appeared to result in a significant degradation of the performance.

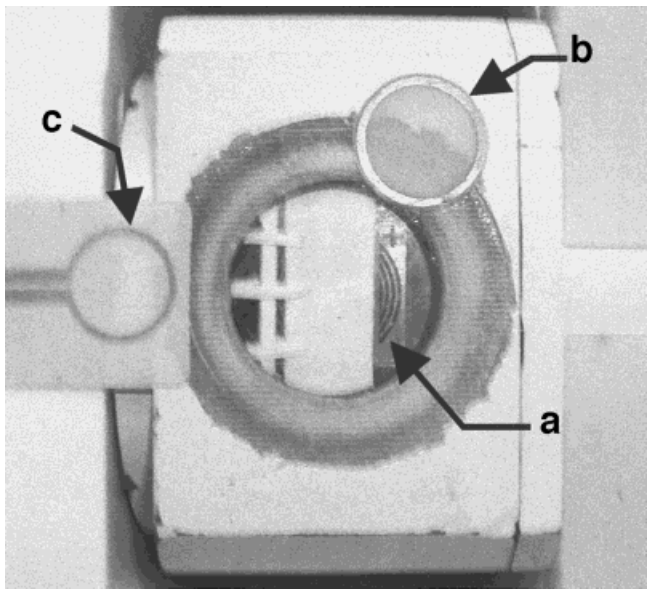

FIG. 4. The HTS resonator (**a**) is placed behind the cryostat window. Fine tuning at 63.835 MHz and matching to the standard preamplifier are achieved by inductively coupling room-temperature copper loops respectively (**b** and **c**).

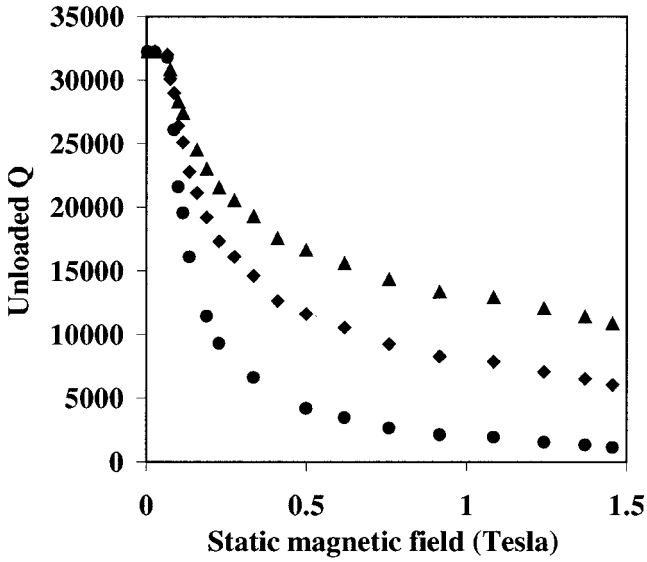

FIG. 5. The unloaded quality factor of the HTS coil as a function of the applied magnetic field, when the field is parallel to the CuO planes (▲), perpendicularly oriented (●), and oriented at 45° (◆).

Prior SNR Estimation

The induction coefficient b_1 of the HTS coil was about 748 μT/A at 2 mm (i.e., the distance due to the cryogenic insulation) on the coil axis. The value of b_1 was 102 μT/A for the copper coil at zero distance from the center coil and 88 μT/A at a 2-mm distance. The data obtained for the HTS and the copper coil are both in good agreement with the theoretical value of b_1 computed using Biot-Savart's law. The variation of b_1 as a function of the distance along the coil axis was found to be similar for both coils.

The internal resistance of the HTS coil at 77 K, corresponding to an unloaded Q of 11000, was about 77 mΩ. The HTS coil had a Q of 1506 outside the magnet when it was placed on the calf, 2 mm away from the coil. The corresponding R_s using Eq. [5] and the unloaded Q of 30000 was 0.53 Ω. There was no significant frequency shift when the coil was loaded. The above measurements indicate that the thermal noise of the HTS coil accounts for approximately 4% of the total noise.

The Q of 101 for the room-temperature copper coil gave an internal resistance of 102 mΩ. The difference between the loaded and unloaded Q values was less than 10%; thus, no values of R_s could be reliably obtained with regard to the accuracy of the measurement. R_s was more accurately estimated (9.8 mΩ) with the help of the HTS-coil data, assuming that the ratio $b_1/\sqrt{R_s}$ was constant due to similar b_1 distributions with the two coils.

The measured value of b_1, R_c, R_s, and Eq. [1] suggest that using the HTS coil for imaging the calf skin should improve the SNR by a factor of 3.2 over that of the room-temperature copper coil.

Clinical Imaging

In vivo images of the calf skin were obtained with the copper coil and with the HTS coil using a single-slice spin-echo sequence with TR/TE = 600/21 msec, a ±6.25 kHz acquisition bandwidth, and a voxel size of 40 × 80 × 900 μm^3 in approximately 10 min. The minimum slice thickness of 0.9 mm was set by the standard gradient capabilities of the MRI system. The acquisition matrix size was 512 × 256. Images were interpolated to 512^2, cropped and displayed on a 512 × 256 matrix.

The image obtained with the HTS coil was of higher quality than the copper-coil image (Fig. 6a and b). The spatial resolution was dramatically improved, so details, such as the fine ramifications connected to the hair follicles, were clearly visible. These ramifications were about 1 or 2 pixels wide, indicating an effective spatial resolution of about 40 μm. Structures with similar signal intensities, such as the papillary dermis, located between the epidermis and the dermis, were also clearly differentiated.

For both images the noise level was about 100, as determined from the standard deviation value measured on a rectangular area of 10000 pixels drawn on the background at the bottom of the images. For each image, three signal profiles were made from the average intensity of a vertical 10-pixel-wide strip: one located at the coil center, and two at half distance from the center to the right and left sides of the image. With the copper coil the mean amplitude of the three profiles was 1730 and 615 in the epidermis and dermis, respectively. With the HTS coil the respective values were 6192 and 2343. This gives an average SNR gain of about 3.6 for the epidermis and 3.8 for the dermis. The deviation in signal amplitude between profiles was within 15% with the HTS coil, while the center profile had a 35% lesser amplitude than outer profiles with the copper coil.

DISCUSSION

Our prior estimation of the SNR obtained by inductive measurements indicated that using a 6-mm-radius HTS coil for imaging the calf skin at 1.5 T could improve the SNR by a factor of 3.2 over that of a room-temperature copper coil. The SNR gain obtained for in vivo images is in quite good agreement with the predicted gain.

Both coils have quite different geometries. Although the b_1 profiles are similar along the coil axis, the radial distribution of b_1 appeared more uniform with the HTS coil than with the copper coil. This may be related to a more uniform current distribution in the plane of the HTS coil provided by the multiturn design. However, the geometry of the copper coil was the most efficient we could achieve using our current RF-coil technology, in terms of $b_1/\sqrt{R_c}$ at the center of the coil. Therefore, our opinion is that the present comparison between both coils is quite fair.

It would be interesting to compare the HTS coil with a cooled copper coil. However, keeping the present geometry of the copper coil would be almost unfair due to the relatively large room needed for the tuning capacitors, and because of the difficulty of ensuring good thermal contact with the cold finger. Implementing a spiral resonator design with copper, such as in the HTS coil, would require dedicated microtechnology to ensure a copper thickness larger than the skin depth (about 10 μm) while keeping the design accurate.

We estimated the theoretical SNR gain we would obtain with the HTS coil over a cooled copper coil (Eqs. [1]–[3]).

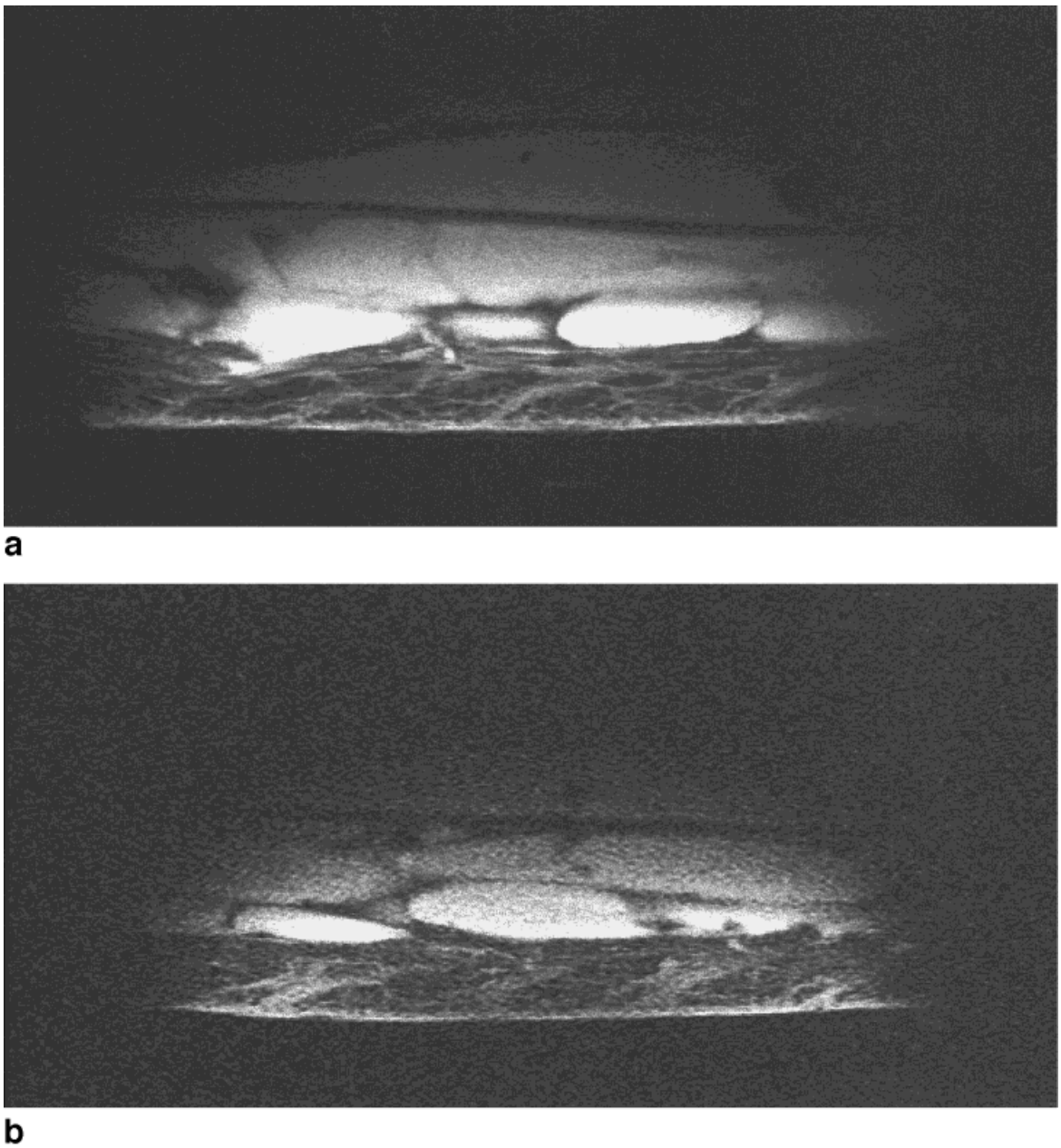

FIG. 6. In vivo images of the calf skin obtained with the (**a**) HTS coil and (**b**) copper coil. The images were obtained using a single-slice spin-echo sequence with TR = 600 msec, TE = 21 msec, a ±6.25 kHz sampling bandwidth, and a voxel size of 40 × 80 × 900 μm^3. The total acquisition time was 10 min.

We also estimated the advantage of using an HTS coil rather than a 77 K copper coil for imaging the skin in anatomical regions other than the calf (either smaller or less conducting). We assumed a sample-induced resistance three times lower than the calf-induced resistance, e.g., that of the finger skin. We also considered smaller coils. The computation was done assuming that b_1 and R_S were inversely and cubically proportional to the coil radius, while R_c was constant as long as the geometrical factor a/r was preserved.

The HTS coil at 77 K would give an SNR that is 1.4-fold better than that of the copper coil at 77 K when imaging the calf skin at 1.5 T (Table 1). Further cooling of the copper coil to 4.2 K would give a similar SNR to the HTS coil at 77 K, since the sample-noise floor would be reached in both cases. Nevertheless, the use of liquid helium would considerably increase the cost and difficulties of implementing the cryostat.

The advantages of the HTS coil are greater with small or poorly conducting samples. Assuming an induced resistance three times lower than the resistance induced by the calf, the HTS coil increases the SNR by a factor of 2 over the copper coil at 77 K. This is illustrated in the work of Wright et al. (10) on finger microimaging at 1.5 T using a cooled copper surface coil. Their copper coil at 77 K had an unloaded Q of 260 and a Q of 250 when loaded by the

Table 1
Evaluation of the SNR for the Copper and the HTS Coils, as a Function of the Coil Size and Temperature and of the Sample Size

		R_cT_c (Ω.K) $\propto T_c\sqrt{\rho(T_c)}$	R_sT_s (Ω.K) $\propto a^3$	b_1 (μT/A) $\propto 1/a$	Normalized SNR (/Cu, 300 K)
Calf skin Coil radius of 6 mm	Copper, 300 K	30.6	3.1	102	1
	Copper, 77 K	2.74	2.3	88	2.2
	Copper, 4.2 K	0.09	2.3	88	3.24
	HTS, 77 K	5.92	166.2	748	3.25
Calf skin Coil radius of 2 mm	Copper, 300 K	30.6	0.115	306	1
	Copper, 77 K	2.74	0.085	264	2.84
	Copper, 4.2 K	0.09	0.085	264	11.4
	HTS, 77 K	5.92	6.15	2244	11.7
Finger skin Coil radius of 6 mm	Copper, 300 K	30.6	1.03	102	1
	Copper, 77 K	2.74	0.77	88	2.59
	Copper, 4.2 K	0.09	0.77	88	5.23
	HTS, 77 K	5.92	55.4	748	5.26

finger. If they had used an HTS coil of equivalent geometry with an unloaded Q 50 times higher than their copper coil, they would have improve their SNR 2.6-fold.

Finally, the HTS coil also appears more attractive when the coil size is reduced. With a threefold size reduction, the HTS coil would provide SNR gains of 4.1 and 11.4 as compared to the copper coil at 77 K and at 300 K, respectively.

HTS coils presently have some drawbacks. A major one is the need to carefully align the superconducting film parallel to the static magnetic field in order to preserve the high Q value. This prevents placing the HTS coil in any orientation within the magnet, and could limit the application range. However, in our experience typical loaded-Q values remained much lower than the observed unloaded-Q value inside the MRI magnet, with no particular attention being taken to avoid slight misalignment ($<5°$) of the coil plane. Another critical point is the tuning of the HTS coil, as it has a very high Q value. The corresponding band pass is then extremely narrow, and tuning must be accurate to account for the additional frequency shifts caused by the static magnetic field. Although the available band pass is wide enough for the experiments presented here, it may be insufficient for much larger acquisition bandwidths or much smaller sample loads. The last major difficulty encountered with surface HTS coils is decoupling the coil during NMR excitation (8,27), which leads to nonuniform flip angle patterns across the image. However, the properties of HTS materials have been, and will continue to be, greatly improved. This should lead to further improvements in coil performance in the presence of an applied magnetic field. On the other hand, dedicated matching-network techniques, such as inductive overcoupling (28), can be developed to overcome the narrow-band pass limitation. Further investigations of coil decoupling schemes during transmission are also worth doing if one considers the great benefits that HTS coils can provide. HTS materials could also provide a way to implement new and much more elaborate designs, such as actively screened RF coils, or highly selective coils providing a much better confinement of the induction coefficient b_1 at the surface of the sample. Indeed, the intrinsically low internal resistance will allow long windings while keeping the sample noise predominant. Finally, the low resistance should allow the coil to be moved away from the body surface so as to further optimize the SNR when the induced resistance decreases more rapidly than b_1 (29,30).

CONCLUSIONS

We have shown that using an HTS coil can provide a significant gain in SNR for in vivo microimaging of the human skin in a 1.5 T whole-body NMR system. The HTS coil performs well at 77 K using a liquid nitrogen cryostat. Calf skin images obtained with the HTS coil show increased SNR and spatial resolution, and will thus be very useful for applications such as the postoperative follow-up of the extent of cutaneous tumors. The improved SNR associated with the high spatial resolution leads to an effective spatial resolution which has never before been obtained on a whole-body NMR scanner. An even higher resolution could be obtained using the HTS coil combined with the high-resolution gradient insert (11) to overcome the standard gradient limitations. Greater SNR gains are expected for smaller or poorer-conducting regions than the calf. There may be other applications for our HTS coil, such as microimaging of nail tumors, studying bone articulations lying near the body surface, studies on small animals, and plant microscopy.

ACKNOWLEDGMENTS

We thank the members of the CIERM (J. Bittoun, director, CHU Bicêtre, France), where the images were obtained, and Thomson-L.C.R. (Corbeville, France) for preparing the HTS coil. The English text was edited by Dr. Owen Parkes.

REFERENCES

1. Hoult DI, Lauterbur PC. The sensitivity of the zeugmatographic experiment involving human samples. J Magn Reson 1979;34:425–433.

2. Hall AS, Alford McNN, Button TW, Gilderdale DJ, Gehring KA, Young IR. Use of high temperature superconductor in a receiver coil for magnetic resonance imaging. Magn Reson Med 1991;20:340–343.
3. VanHeteren JG, James TW, Bourne LC. Thin film high temperature superconducting RF coils for low-field MRI. Magn Reson Med 1994;32: 396–400.
4. Vester M, Steinmeyer F, Roas B, Thummes G, Klundt K. High temperature superconducting surface coils with liquid nitrogen or pulse tube refrigeration. In: Proceedings of the 5th Annual Meeting of ISMRM, Vancouver, Canada, 1997. p 1528.
5. Black RD, Early TA, Roemer PB, Mueller OM, Mogro-Campero A, Turner LG, Johnson GA. A high-temperature superconducting receiver for nuclear magnetic resonance microscopy. Science 1993;259:793–795.
6. Black RD, Early TA, Johnson GA. Performance of high-temperature superconducting resonator for high-field imaging. J Magn Reson 1995; 113:74–80.
7. Odoj F, Rommel E, Kienlin MV, Haase A. A superconducting probe head applicable for nuclear magnetic resonance microscopy at 7 T. Rev Sci Instrum 1998;69:2708–2712.
8. Miller JR, Hurlston SE, Ma QY, Face DW, Kountz DJ, MacFall JR, Hedlund LW, Johnson GA. Performance of a high-temperature superconducting probe for in-vivo microscopy at 2.0 T. Magn Reson Med 1999;41:72–79.
9. Hurltson SE, Brey WW, Suddarth SA, Johnson GA. A high temperature superconducting helmholtz probe for microscopy at 9.4 T. Magn Reson Med 1999;41:1032–1038.
10. Wright AC, Song HK, Wehrli FW. In vivo MR micro imaging with conventional radiofrequency coils cooled at 77°K. Magn Reson Med 2000;43:163–169.
11. Bittoun J, Saint-Jalmes H, Querleux BG, Darrasse L, Jolivet O, Idy-Peretti I, Wartski M, Richard SB, Lévêque JL. In vivo high-resolution MR imaging of the skin in a whole-body system at 1.5 T. Radiology 1990;176:457–460.
12. Ginefri J-C, Darrasse L, Crozat P. Correlation between radiofrequency and microwave superconducting properties of YBaCuO dedicated to magnetic resonance imaging. IEEE Trans Appl Supercond 1999;9: 4695–4701.
13. Chen CN, Hoult DI. Biomedical magnetic resonance technology. New York: Adam Hilger; 1989.
14. Hoult DI, Richards RE. The signal-to-noise ratio of the nuclear magnetic resonance experiment. J Magn Reson 1976;24:71–85.
15. Powel RL, Ficket FR. Cryogenic properties of copper. National Bureau of Standards, Boulder, Colorado.
16. Gabriel S, Lau RW, Gabriel C. The dielectric properties of biological tissues: II. Measurements in the frequency range 10 Hz to 20 GHz. Phys Med Biol 1996;41:2251–2269.
17. Sauzade M, Darrasse L. Sensitivity in NMR imaging. International Workshop on Measurement, Smolenice, Slovakia, 1993.
18. Serfaty S, Haziza N, Darrasse L, Kan S. Multi-turn split conductor parallel plate resonator. In: Proceedings of the 4th Annual Meeting of ISMRM, New York, 1996. p 1428.
19. Lemaître Y, Mercanralli LM, Dessertenne B, Mansart D, Marcilhac B, Mage JC. Large-area high-quality YBCO thin films by inverted cylindrical magnetron technique. Physica C 1994;235–240:643–644.
20. Bohn CL, Delayen JR, Dos Santos DI, Lanagan MT, Shepard KW. RF properties of high-TC superconductors. IEEE Trans Magn 1989;25: 2406–2409.
21. Sonier JE, Kiefl RF, Brewer JH, Bonn DA, Dunsiger SR, Hardy WN, Ruixing L, Macfarlane WA, Riseman TM, Noakes DR, Stronach CE. Magnetic field dependence of the London penetration depth in the vortex state of YBaCuO. Phys Rev B 1997;55:11789–11792.
22. Hübner H, Valenzuela AA. Radiofrequency performances of superconducting thin films in high magnetic fields. Appl Phys Lett 1994;64: 3491–3493.
23. Hoult DI. Magnetic resonance in biology. New York: Wiley; 1980.
24. Ginefri J-C, Durand E, Darrasse L. Quick measurement of NMR coil sensitivity with a single-loop probe. Rev Sci Instrum 1999;70:4730–4731.
25. Darrasse L, Kassab G. Quick measurement of NMR-coil sensitivity with a dual-loop probe. Rev Sci Instrum 1993;64:1841–1844.
26. Song HK, Wehrli FW, Ma J. In vivo MR microscopy of the human skin. Magn Reson Med 1997;37:185–191.
27. Bendal MR, Connelly A, McKendry JM. Elimination of coupling between cylindrical transmit coils and surface-receive coils for in vivo NMR. Magn Reson Med 1986;3:157–163.
28. Raad A, Darrasse L. Optimization of NMR receiver bandwidth by inductive coupling. Magn Reson Imaging 1992;10:55–65.
29. Serfaty S, Darrasse L, Kan S. The pinpoint NMR coil. In: Proceedings of the 2nd Annual Meeting of SMR, San Francisco, 1994. p 219.
30. Ginefri J-C, Darrasse L, Crozat P. In-vivo human skin microscopy using a superconducting receiver coil. In: Proceedings of the 7th Annual Meeting of ISMRM, Philadelphia, 1999. p 2129.